

SYNTHESIS AND CHARACTERIZATION OF EFB CLINKER SUPPORTED NICKEL AND COBALT CATALYSTS FOR METHANE DRY REFORMING

CHAN HAN JIE

Thesis submitted in partial fulfilment of the requirements
for the award of the degree of
Bachelor of Chemical Engineering

**Faculty of Chemical & Natural Resources Engineering
UNIVERSITI MALAYSIA PAHANG**

JANUARY 2015

©CHAN HAN JIE (2015)

ABSTRACT

Methane dry reforming is environmental friendly due to the potential sequestration of CO₂. Therefore, substantial research works have been carried out to develop reforming catalysts that exhibit high catalytic performance and excellent longevity. The current work reports on the synthesis of 20wt%Co/80wt%EFB clinker and 20wt%Ni/80wt%EFB clinker catalysts via wet-impregnation technique, followed by various characterization techniques such as BET, XRD, XRF, TGA and FESEM. The BET specific surface area of Co/EFB clinker and Ni/EFB clinker catalyst were 2.83 m²g⁻¹ and 2.37 m²g⁻¹, respectively. In addition, XRD diffractogram of EFB clinker showed two highest peaks at around $2\theta = 27.2^\circ$ and 31.5° , which can be attributed to CaO and K₂O species, respectively. This finding was also consistent with XRF analysis where potassium (K) and calcium (Ca) were positively identified. Subsequently, methane dry reforming studies revealed that Ni/EFB clinker catalyst always yielded higher formation rates of H₂ and CO. Indeed, the rate was maximum at CO₂:CH₄ feed ratio of unity. The average conversion of CH₄ for reactions using Co/EFB clinker and Ni/EFB clinker catalyst are obtained to be 78.26 % and 78.19 % respectively. Meanwhile, the average conversion of CO₂ for reactions using Co/EFB clinker and Ni/EFB clinker catalyst are 80.40 % and 81.17 % respectively. When reaction temperatures were varied, the activation energy over Co/EFB clinker was 124.4 kJ mol⁻¹ while that for the reaction over the Ni/EFB clinker catalyst was 113.0 kJ mol⁻¹. Post reforming reaction, oxidation profiles of the used catalysts indicated carbon-free condition. This was corroborated by the FESEM images for both sets of used catalysts, where no carbon whisker was found.

ABSTRAK

Tindak balas metana dan karbon dioksida merupakan satu proses yang mesra alam. Oleh itu, banyak penyelidikan telah dijalankan bagi menghasilkan pemangkin yang berprestasi tinggi dan berhayat panjang. Kerja ini bertujuan untuk menghasilkan pemangkin yang berasaskan Ni dan Co yang disokong oleh klinker tandan buah sawit melalui kaedah impregnasi basah dengan formulasi yang 20-80. Pelbagai teknik pencirian seperti BET, XRD, XRF, TGA, FESEM dan EDX telah digunakan untuk mendapatkan ciri-ciri pemangkin yang dihasil. Kajian BET mendapati bahawa kawasan permukaan tertentu BET untuk pemangkin Co/EFB klinker dan Ni/EFB klinker adalah $2.83 \text{ m}^2\text{g}^{-1}$ and $2.37 \text{ m}^2\text{g}^{-1}$ masing-masing. Di samping itu, diffractogram XRD EFB klinker menunjukkan dua puncak di $2\theta = 27.2^\circ$ dan 31.5° , yang boleh dikaitkan dengan spesis CaO dan K_2O . Carian ini juga konsisten dengan analisis XRF iaitu kalium (K) dan kalsium (Ca) dapat dikenal pasti secara positif. Selain itu, kajian tindak balas metana dan karbon dioksida mendedahkan bahawa pemangkin Ni/EFB klinker sentiasa menghasilkan kadar penghasilan H_2 dan CO yang lebih tinggi. Sesungguhnya, kadar itu adalah maksimum pada $\text{CO}_2:\text{CH}_4$ bernisbah 1:1. Penukaran purata CH_4 untuk tindak balas menggunakan pemangkin Co/EFB klinker dan Ni/EFB klinker didapati ialah 78.26% dan 78.19% masing-masing. Sementara itu, penukaran purata CO_2 untuk tindak balas menggunakan pemangkin Co/EFB klinker dan Ni/EFB klinker didapati ialah 80.40% dan 81.17% masing-masing. Apabila suhu tindak balas telah diubah, tenaga pengaktifan bagi Co/EFB klinker adalah 124.4 kJmol^{-1} manakala bagi tindak balas yang pakai pemangkin Ni/EFB klinker adalah 113.0 kJmol^{-1} . Kedua-dua pemangkin yang telah dipakai digunakan untuk menjalankan analisis profil pengoksidaan. Analisis bagi kedua-dua pemangkin mendapati bahawa kedua-dua set pemangkin yang diguna tidak menghadapi masalah pemendapan karbon yang kritikal.

TABLE OF CONTENTS

SUPERVISOR'S DECLARATION	IV
STUDENT'S DECLARATION	V
<i>Dedication</i>	VI
ACKNOWLEDGEMENT	VII
ABSTRACT.....	VIII
ABSTRAK.....	IX
TABLE OF CONTENTS.....	X
LIST OF FIGURES	XII
LIST OF TABLES	XIV
LIST OF ABBREVIATIONS.....	XV
LIST OF ABBREVIATIONS.....	XVI
1 INTRODUCTION	1
1.1 Background	1
1.2 Problem Statement and Motivation.....	2
1.3 Objective	3
1.4 Scopes	3
1.5 Outline of Thesis	4
2 LITERATURE REVIEW	5
2.1 General Overview	5
2.2 Steam Reforming Reaction Process	5
2.3 Dry Reforming Reaction Process	5
2.4 Reactions in methane dry reforming	6
2.5 Reforming Catalyst	8
2.6 Catalyst Preparation	14
2.7 Catalyst Deactivation	15
2.8 Summary	17
3 MATERIALS AND METHODS.....	18
3.1 Materials.....	18
3.2 Catalyst Physicochemical Characterization	18
3.2.1 <i>Brunauer-Emmett-Teller (BET)</i>	19
3.2.2 <i>X-ray Diffraction (XRD)</i>	21
3.2.3 <i>Field Emission Scanning Electron Microscopy (FESEM)</i>	23
3.2.4 <i>Energy-dispersive X-ray Spectroscopy (EDX)</i>	24
3.2.5 <i>Thermo gravimetric analysis (TGA)</i>	25
3.2.6 <i>X-ray Fluorescence (XRF)</i>	27
3.3 Catalyst reaction.....	28
4 RESULTS AND DISCUSSIONS.....	30
4.1 Catalyst Preparation	30
4.2 Fresh Catalyst Characterization	31
4.2.1 <i>X-ray Fluorescence (XRF)</i>	31
4.2.2 <i>XRD</i>	32
4.2.3 <i>Liquid N₂ Physisorption (BET)</i>	33
4.2.4 <i>Thermogravimetric Analysis (TGA)</i>	36
4.2.5 <i>FESEM Imaging</i>	38
4.2.6 <i>Energy-dispersive X-ray Spectroscopy (EDX)</i>	38

4.3	Dry Reforming Reaction Studies	39
4.3.1	<i>Mass Transfer Limitation Studies</i>	39
4.3.2	<i>Catalyst Performance</i>	40
4.3.3	<i>Effect of Feed Ratio and Reaction Temperature</i>	43
4.3.4	<i>Longevity Study</i>	49
4.4	Used Catalyst Characterization	51
4.4.1	<i>Thermogravimetric analysis (TGA)</i>	51
4.4.2	<i>FESEM Imaging</i>	52
4.4.3	<i>Energy Dispersive X-ray spectrometry (EDX)</i>	53
5	CONCLUSIONS AND RECOMMENDATIONS	54
5.1	Conclusions	54
5.2	Recommendations	54
	REFERENCES	56
	APPENDIX A	60
	APPENDIX B	61
	APPENDIX C	79

LIST OF FIGURES

Figure 2.1: Equilibrium constants of reactions involving in CH ₄ -CO ₂ reaction at different temperatures and atmospheric pressure (Source: Nikoo and Amin, 2011).....	7
Figure 2.2: Carbon deposition as a function of temperature and CO ₂ /CH ₄ ratio	16
Figure 3.1: Deriving Bragg's Law using the reflection geometry and applying trigonometry.....	21
Figure 3.2: Schematic diagram of a general Field Emission SEM.....	23
Figure 3.3: Schematic diagram of EDX	24
Figure 3.4: Schematic diagram of TGA	26
Figure 3.5: Schematic diagram of XRF	28
Figure 3.6: Experimental Setup	29
Figure 4.1: XRD spectra of Co/EFB clinker catalyst, Ni/EFB clinker catalyst and EFB clinker	32
Figure 4.2: Isotherm plot of (a) EFB clinker, (b) Co/EFB clinker and (c) Ni/EFB clinker	35
Figure 4.5: Weight (%) versus Temperature (K) over both catalysts at 20 K min ⁻¹	36
Figure 4.6: Weight profile (%) versus Temperature (K) over (a) Co/EFB clinker and (b) Co/EFB clinker catalyst at different ramping rate (10, 15 and 20 K min ⁻¹)	37
Figure 4.8: SEM image of (a) fresh EFB clinker support, (b) fresh Co/EFB clinker catalyst and (c) fresh Ni/EFB clinker catalyst	39
Figure 4.9: EDX of (a) 20wt% Co/EFB clinker catalyst (b) 20wt% Ni/EFB clinker ...	38
Figure 4.10: Transient profile of conversion of CH ₄	41
Figure 4.11: Average conversion of CH ₄ and CO ₂ for the catalyst tested in the dry reforming of methane. (T = 1173K; P = 1atm; CO ₂ : CH ₄ = 1)	42
Figure 4.12: Rate of formation for both H ₂ and CO.....	43
Figure 4.13: Average conversion of CH ₄ for the catalyst tested in the dry reforming of methane for various feed ratio. (T = 1173K; P = 1atm)	44
Figure 4.14: (a) Rate of consumption of CH ₄ (b) Rate of formation of H ₂ versus various feed ratio. (T = 1173K; P = 1atm)	45
Figure 4.15: Rate of consumption of CH ₄ versus temperature (P = 1atm; CO ₂ : CH ₄ = 1)	46
Figure 4.16: Rate of formation of H ₂ versus temperature (P = 1atm; CO ₂ : CH ₄ = 1) ...	47
Figure 4.17: Rate of formation of CO versus temperature (P = 1atm; CO ₂ : CH ₄ = 1)..	47
Figure 4.18: Rate of formation of H ₂ and CO and rate of consumption of CH ₄ with various temperatures for Co/EFB clinker catalyst	48
Figure 4.19: Rate of formation of H ₂ and CO and rate of consumption of CH ₄ with various temperatures for Ni/EFB clinker catalyst.....	49
Figure 4.20: Transient Profiles of CH ₄ Conversion.....	50

Figure 4.21: Weight change (%) versus temperature (K).....	51
Figure 4.22: FESEM image of spent Co/EFB clinker catalyst.....	52
Figure 4.23: FESEM image of spent Ni/EFB clinker catalyst.....	52
Figure 4.24: EDX of spent Co/EFB clinker catalyst	53
Figure 4.25: EDX of spent Ni/EFB clinker catalyst	53

LIST OF TABLES

Table 2.1: Reaction in CO ₂ reforming of methane (Source: Nikoo and Amin, 2011)	6
Table 2.2: Summary of previous research and its significant result	9
Table 3.1: List of chemical and its purity	18
Table 3.2: List of gases and its purity	18
Table 4.3: XRF Results.....	31
Table 4.1: Crystallite size determined for the peak around $2\theta = 37.01^\circ$ for Co/EFB clinker catalyst and $2\theta = 43.38^\circ$ for Ni/EFB clinker catalyst.	33
Table 4.2: BET specific surface area and pore volume of sample.....	35
Table 4.4: Average Conversion of CH ₄ and CO ₂	41
Table 4.5: Activation Energy table	48

LIST OF ABBREVIATIONS

- a : effective cross-sectional area of one adsorbate molecule
 C : dimensionless constant that related to the enthalpy adsorption of adsorbate gas
 d : spacing between layers of atoms
 D : crystalline size
 E_a : activation energy
 K : dimensionless shape factor
 k_{Sch} : Scherrer constant
 n : order of reflection (integer)
 P : partial vapour pressure of adsorbate gas in equilibrium
 P_0 : saturated pressure of adsorbate gas
 P/P_0 : relative pressure
 R : gas constant
 T : temperature
 V_a : volume of gas adsorbed at STP
 V_M : volume of gas adsorbed corresponding to monolayer coverage

Greek

- (ΔG_r) : Gibbs free energy change of reaction
 λ : wavelength
 β : line broadening at half the maximum intensity
 θ : Bragg angle

LIST OF ABBREVIATIONS

BET	Brunauer-Emmett-Teller
BOD	Biochemical Oxygen Demand
COD	Chemical Oxygen Demand
GDP	Gross Domestic Product
EDX	Energy Dispersive X-ray Spectroscopy
EFB	Empty Fruit Bunch
FESEM	Field Emission Scanning Electron Microscopy
OPF	Oil Palm Fronds
OPT	Oil Palm Trunks
POME	Palm Oil Mill Effluent
SEM	Scanning Electron Microscope
STP	Standard temperature and pressure
TGA	Thermogravimetric Analysis
XRD	X-ray Diffraction

1 INTRODUCTION

1.1 Background

Synthesis gas is a fuel gas mixture comprised of CO and H₂. It is a vital feedstock for downstream petrochemical industries i.e. gasoline, ammonia, methanol etc. As the world grapples with potentially-devastating energy crunch situation, renewable energy such as synthesis gas has been touted as a potential saviour.

Significantly, in Malaysia palm oil mill effluent or also known as POME is a highly polluting wastewater with high chemical oxygen demand (COD) and biochemical oxygen demand (BOD) (Lam & Lee, 2011). Under ambient conditions, degradation of POME usually releases a large amount of CH₄ and CO₂ (collectively known as biogas) into the atmosphere, which may worsen the global warming (Schuchardt et al., 2008). Carbon dioxide (CO₂) has been identified as one of the most significant greenhouse gases arising from anthropogenic activities. Hence, mankind needs to curb CO₂ emissions in order to counteract global warming (Er-rbib et al., 2012). One of the propositions is to utilize CH₄ and CO₂ simultaneously via dry (CO₂) reforming pathway. The dry reforming of methane results in product with a lower H₂:CO ratio (< 2.0) which is more favourable for olefins or methanol synthesis compared to the yield from the conventional steam reforming which normally produces H₂:CO ratios > 3.0 (Siahvashi & Adesina, 2013). Besides, the use of CO₂ as co-reactant has also attracted growing attention due to the potential sequestration of CO₂ and energy savings (Siahvashi & Adesina, 2013).

Indeed, catalysts play a vital role in the aforementioned reaction. Catalyst is usually comprised of active metal and support. A supporter is usually a solid with a high surface area, to which a catalyst is affixed. Relentless efforts have been dedicated to maximize the surface area of a catalyst by distributing it over the support (McNaught & Wilkinson, 2014). Previous studies and reviews have been published on the Ni based metal with different supported catalysts employed in the light hydrocarbon dry reforming. An evaluative investigation of propane CO₂ reforming over bimetallic alumina supported 5%Mo-10%Ni catalyst has been carried out in a fixed bed reactor at 0.1 M Pa and temperatures ranging from 823 – 973K. It was found that Mo-Ni is a stable and active

catalyst at different temperature during the dry reforming process (Siahvashi et al., 2013). Besides, numerous supported catalysts have been tested, especially Ni- and noble metal-based catalysts, and they have been found to exhibit promising catalytic performance. Conversion of CH_4 and CO_2 to synthesis gas, approaching those defined by thermodynamic equilibrium, can be obtained over the aforementioned catalysts as long as sufficient contact times are maintained.

One of the major problems encountered during dry reforming is the deactivation of the catalysts due to carbon deposition. To alleviate the deactivation problem arising from Ni catalysts coking, it has been shown that addition of alkali or alkaline earth oxide to the Ni based catalyst lead to drastic decrease in the number of sites for carbon formation, while sufficiently maintaining the active sites for the reforming (Lemonidou et al., 1998). From the EDX result of EFB clinker, it was found that EFB has a basic characteristic and it should be suitable to act as the supporter for the Ni-based and Co-based catalysts.

1.2 Problem Statement and Motivation

Oil palm is the most important commodity from Malaysia with significant contribution to its gross domestic product (GDP). Lignocellulosic biomass which is produced from the oil palm industries include parts such as oil palm trunks (OPT), oil palm fronds (OPF), empty fruit bunches (EFB) and palm oil mill effluent (POME). Nevertheless, the presence of these oil palm wastes has created a major disposal problem (Abdullah & Sulaiman, 2013). EFB are the main source of biomass that could be utilized by the power plant due to its ready-availability as daily biomass-waste. Most of the plantations use a small fraction of this EFB waste for internal use, with a large portion being put aside for either biodegrading into compost, or at times burnt to avoid space loss by storage (Matt et al., 2014). As a fuel, EFB is burnt in a furnace to generate heat and electricity for sustaining palm oil mill operation. The residue from this process is what is known as EFB clinker whereby it will be adopted for the first time in this work as supporter for Ni catalyst for methane dry reforming reaction. Most of the previous studies primarily investigated the development of catalyst for high catalytic performance and stability. Therefore, an optimum conversion of synthesis gas can be achieved. However, most of these works did not focus on the environment impact of the catalyst. To illustrate, an evaluative investigation of propane CO_2 reforming over bimetallic alumina supported 5%Mo-

10%Ni catalyst sounds promising in dry reforming (Siahvashi et al., 2013). In fact, calcium aluminate has been proven to be active with lower coke deposition for the reaction of reforming (Lemonidou et al., 1998). From the characterisation of EFB clinker, high percentage of K and Ca were found. Hence it is believed to be basic. A basic catalyst can reduce back pressure in the packed bed column as carbon deposition will be reduced substantially (Ranjbar & Rezaei, 2012b). Last but not least, it is worth to explore the possibility of this palm oil industries waste as catalyst supporter in this study.

1.3 Objective

This research work is carried out to synthesize and characterize EFB clinker supported 20wt% Co and 20wt%Ni catalysts for methane dry reforming studies at atmospheric pressure.

1.4 Scopes

In order to achieve the outlined objective of this work, the following scopes have been identified:

i) **Catalysts Preparation:**

The 20wt%Co/80wt%EFB and 20wt%Ni/80wt%EFB catalysts were prepared via wet-impregnation method.

ii) **Catalyst Characterisation:**

The methods applied in this study were BET, XRD, XRF, TGA, FESEM and EDX. BET was used to find out the specific surface area, pore volume and pore size distribution sample of catalysts. The crystalline structure and the size of crystallite diameter were determined via XRD. Besides, XRF was employed for analysis of major and trace elements in the EFB clinker. The catalyst-gas interaction profile was obtained from TGA instrument. In addition, TGA also allowed the determination of coke location as well. Lastly, the image of coke deposit structure at the sample catalysts can be observed via FESEM while EDX shows the composition of element that contained in the sample catalysts.

iii) Catalyst Reaction:

The catalytic screening was carried out by placing 0.3 g of catalyst into the stainless steel fixed-bed reactor (ID: 10 mm) supported by two layers of quartz wool. The feed comprised of the CH₄ and CO₂ mixture at equal proportion and the reaction temperature was set at 1173 K for catalyst screening studies. Subsequently, the CO₂ to CH₄ ratios and temperatures were varied between 1073 – 1173 K to determine the ratio of product produced by the best catalyst.

1.5 Outline of Thesis

This thesis is divided into four chapters. Chapter 1 describes the problem statements that motivate the current work. In the same chapter, the objective and scopes of the study are presented. Chapter 2 reviews the background of the study and describes previous works of other researchers. The materials and methodology used in the study and design of the experiments are discussed in Chapter 3. In Chapter 4, experimental results include characterization analysis and some kinetics modelling will be presented. Finally, the conclusions and some recommendations of this thesis and outlook for future work are summarized in Chapter 5.

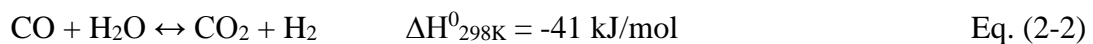
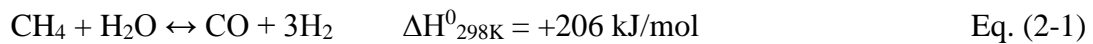
2 LITERATURE REVIEW

2.1 General Overview

Dry (CO₂) reforming of methane is a well-studied reaction that is of both scientific and industrial importance. This reaction produces syngas that can be used to produce wide range of products especially in downstream petrochemical processes. Conventional production of syngas is via natural gas steam reforming. However, fossil hydrocarbons resources are decreasing in the face of growing demand from developing countries; hence a sudden spike in energy price. In lieu of this, synthesis gas availability as an alternative fuel source (via Fischer-Tropsch synthesis) in addition to the aforementioned processes is clearly desirable. In this section, previous studies related to the reforming reaction, related catalysts, as well as coke deactivation phenomenon are presented.

2.2 Steam Reforming Reaction Process

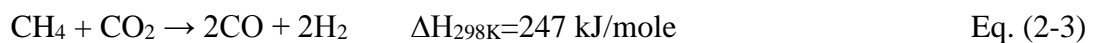
The most established process for syngas production is natural gas/ methane steam reforming. This reaction is endothermic and takes place at temperature above 1123 K. The reforming reaction can be represented as:



For the steam reforming reaction, the production of hydrogen increased with pressure because the forward water-gas shift reaction produced additional hydrogen by the reaction of CO with water (Oyama et al., 2012).

2.3 Dry Reforming Reaction Process

The methane dry reforming is a highly endothermic reaction and the reaction occurs at 1073-1073 K at atmospheric pressure. Theoretically, the process has a unity molar ratio for H₂/CO. The reforming reaction can be represented as:



For the production of synthesis gas and hydrogen, the dry reforming have an environmental benefit as it consumes CO₂. However, there are some drawbacks of dry

reforming methane, *viz.* catalyst sintering at high temperature, a possibly lower H₂/CO ratio compared to steam reforming attributed to the reverse water-gas shift reaction (Oyama et al., 2012) and catalyst deactivation due to carbon deposition from either methane cracking (CH₄ ↔ C + 2H₂) or Boudouard reaction (2CO ↔ C + CO₂). Therefore, the production of hydrogen via dry reforming appears to be a weak competitor for the steam reforming. Nonetheless, the production of synthetic fuels is interesting prospect for valorization of CO₂. Indeed, this alternative consumes CO₂ as well (Er-rbib et al., 2012).

2.4 Reactions in methane dry reforming

Table 2.1 shows the main reactions which may occur in CO₂ reforming of methane.

Table 2.1: Reaction in CO₂ reforming of methane (Source: Nikoo and Amin, 2011)

Reaction	ΔH_{298} (kJ/mol)	Reaction number
$CH_4 + CO_2 \leftrightarrow 2CO + 2H_2$	247	(1)
$CO_2 + H_2 \leftrightarrow CO + H_2O$	41	(2)
$2CH_4 + CO_2 \leftrightarrow C_2H_6 + CO + H_2O$	106	(3)
$2CH_4 + 2CO_2 \leftrightarrow C_2H_4 + 2CO + 2H_2O$	284	(4)
$C_2H_6 \leftrightarrow C_2H_4 + H_2$	136	(5)
$CO + 2H_2 \leftrightarrow CH_3OH$	-90.6	(6)
$CO_2 + 3H_2 \leftrightarrow CH_3OH + H_2O$	-49.1	(7)
$CH_4 \leftrightarrow C + 2H_2$	74.9	(8)
$2CO \leftrightarrow C + CO_2$	-172.4	(9)
$CO_2 + 2H_2 \leftrightarrow C + 2H_2O$	-90	(10)
$H_2 + CO \leftrightarrow H_2O + C$	-131.3	(11)
$CH_3OCH_3 + CO_2 \leftrightarrow 3CO + 3H_2$	258.4	(12)
$3H_2O + CH_3OCH_3 \leftrightarrow 2CO_2 + 6H_2$	136	(13)
$CH_3OCH_3 + H_2O \leftrightarrow 2CO + 4H_2$	204.8	(14)
$2CH_3OH \leftrightarrow CH_3OCH_3 + H_2O$	-37	(15)
$CO_2 + 4H_2 \leftrightarrow CH_4 + 2H_2O$	-165	(16)
$CO + 3H_2 \leftrightarrow CH_4 + H_2O$	-206.2	(17)

The equilibrium constants of all reactions that are supposed to occur are exhibited as a function of temperature in Figure 2.1. According to the thermodynamic principles, when the Gibbs free energy change of reaction (ΔG_r) is negative (larger Ln (K)), the reaction is spontaneous. In contrast, for positive ΔG_r (smaller Ln (K)), the reaction is thermodynamically limited (Smith et al., 2005). As shown in Figure 2.1, CO₂ reforming of methane (reaction 1: CH₄ + CO₂ ↔ 2CO + 2H₂) to form syngas is a favourable reaction,

particularly at a temperature >1000 K, consistent with the suggested temperature range in the previous study (Istadi et al., 2005). Reverse water gas-shift (RWGS) as numbered as reaction 2 ($\text{CO}_2 + \text{H}_2 \leftrightarrow \text{CO} + \text{H}_2\text{O}$) is much affected by equilibrium within the entire investigated temperature range. In general, CO_2 reforming of methane is typically accompanied by simultaneous occurrence of RWGS reaction.

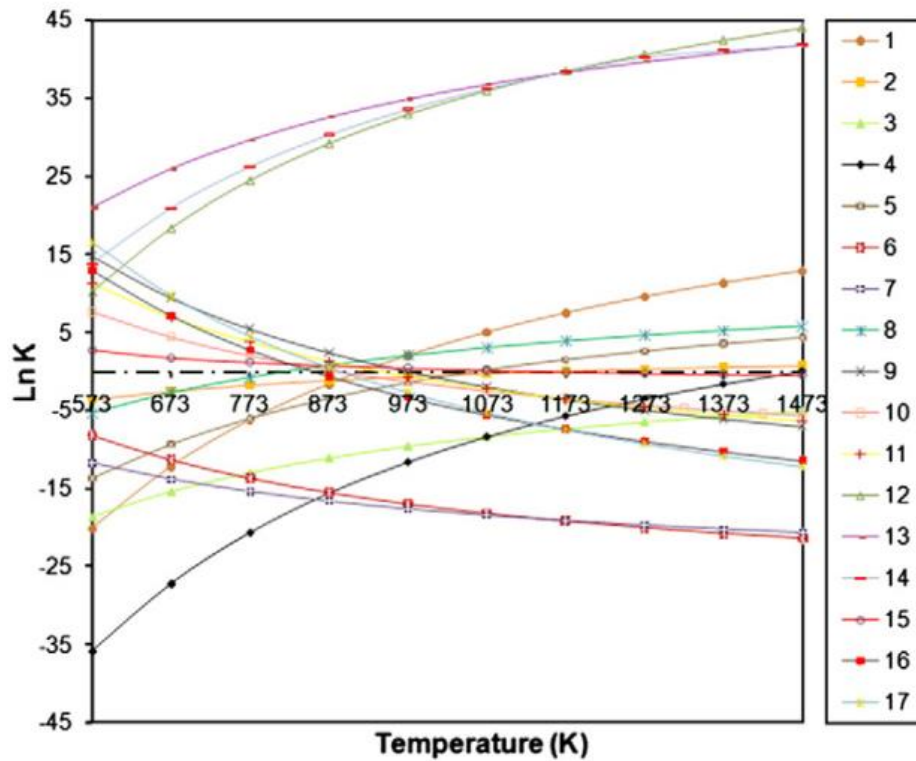


Figure 2.1: Equilibrium constants of reactions involving in $\text{CH}_4\text{-CO}_2$ reaction at different temperatures and atmospheric pressure (Source: Nikoo and Amin, 2011)

The oxidative coupling of methane reactions (reaction 3 and 4: $2\text{CH}_4 + \text{CO}_2 \leftrightarrow \text{C}_2\text{H}_6 + \text{CO} + \text{H}_2\text{O}$ and $2\text{CH}_4 + 2\text{CO}_2 \leftrightarrow \text{C}_2\text{H}_4 + 2\text{CO} + 2\text{H}_2\text{O}$) are not feasible except at a very high temperature due to the high negative values of $\text{Ln}(K)$. Dehydrogenation of ethane (reaction 5: $\text{C}_2\text{H}_6 \leftrightarrow \text{C}_2\text{H}_4 + \text{H}_2$) has the enough tendency to occur at higher temperature for ethylene production, although the reaction can be also affected by equilibrium limitations. Hydrogenation of CO_2 and CO (reaction 6 and 7: $\text{CO} + 2\text{H}_2 \leftrightarrow \text{CH}_3\text{OH}$ and $\text{CO}_2 + 3\text{H}_2 \leftrightarrow \text{CH}_3\text{OH} + \text{H}_2$) is much favourable towards the reverse side, especially at high temperatures, as their $\text{Ln}(K)$ are negative.

Carbon may be formed via methane decomposition (reaction 8: $\text{CH}_4 \leftrightarrow \text{C} + 2\text{H}_2$), disproportionation (reaction 9: $2\text{CO} \leftrightarrow \text{C} + \text{CO}_2$) (Froment, 2000), hydrogenation of

carbon dioxide (reaction 10: $\text{CO}_2 + 2\text{H}_2 \leftrightarrow \text{C} + 2\text{H}_2\text{O}$) and hydrogenation of carbon monoxide (reaction 11: $\text{H}_2 + \text{CO} \leftrightarrow \text{H}_2\text{O} + \text{C}$), although these reactions are affected by the change in molar ratio of reactants due to their low $\ln(K)$ within the investigated temperature range. Reaction 8 is more probable for carbon formation at the higher temperature, whereas all three other reactions (reactions 9 – 11) tend to generate carbon at lower temperature (<800 K) and can be influenced by equilibrium limitations at the higher temperature. Reaction 12 ($\text{CH}_3\text{OCH}_3 + \text{CO}_2 \leftrightarrow 3\text{CO} + 3\text{H}_2$), reaction 13 ($3\text{H}_2\text{O} + \text{CH}_3\text{OCH}_3 \leftrightarrow 2\text{CO}_2 + 6\text{H}_2$) and reaction 14 ($\text{CH}_3\text{OCH}_3 + \text{H}_2\text{O} \leftrightarrow 2\text{CO} + 4\text{H}_2$) however, can be improved and shifted towards the right-hand side within the whole considered temperature range, while reaction 15 ($2\text{CH}_3\text{OH} \leftrightarrow \text{CH}_3\text{OCH}_3 + \text{H}_2\text{O}$) is easily influenced by equilibrium limitations. The composition of the products can be greatly varied for those reaction with $\ln(K)$ are in the vicinity of zero within the considered temperature range. The methanation, reaction 16 ($\text{CO}_2 + 4\text{H}_2 \leftrightarrow \text{CH}_4 + 2\text{H}_2\text{O}$) and 17 ($\text{CO} + 3\text{H}_2 \leftrightarrow \text{CH}_4 + \text{H}_2\text{O}$) can occur at lower temperature (<800 K) with positive magnitude of $\ln(K)$, but are restricted at the high temperature due to their negative $\ln(K)$ and both reactions being exothermic (Nikoo and Amin, 2011).

2.5 Reforming Catalyst

Study on the catalyst development of this reaction has been focused on screening a new catalyst to reach higher activity and better stability toward sintering, carbon deposition (coking), metal oxidation, and forming of inactive chemical species (Budiman et al., 2012). Numerous scientific publications reported that all members of group VIII transition metals with exception of Osmium especially Ni, Ru, Rh, Pd, Ir and Pt exhibited activity to this type of reaction (Ferreira-Aparicio et al., 2005). Nevertheless, based on economical view, upscale toward industrial level of noble metals is not suitable considering their high cost and restricted availability.

Nickel (Ni) based catalyst is commonly studied because of its low cost and availability. Although supported nickel catalyst has high effectiveness at elevated reaction temperatures, carbon deposition remains an issue that impede its widespread use. Carbon deposition which may form on the catalyst surface and/or the tubes of the reactor could lead to deactivation of the catalyst and/or plugging of the tubes (Budiman et al., 2012). Because of this, it is impossible to avoid carbon formation under low or unity CO_2/CH_4

ratios using nickel catalyst (Chen et al., 2001). Recently, even though not a focus of attention, it has been revealed that the supported cobalt catalyst shows considerable activity for dry reforming of methane process (Wang and Ruckenstein, 2000). Although the catalytic performance, such as activity is neither superior to nickel nor to the noble metal catalyst, study on the supported cobalt catalyst were also reported to find out the better catalytic performance (Ferreira-Aparicio et al., 2005). It is also probable that the mechanism of carbon deposition on cobalt metal is different from that of nickel metal. Cobalt catalyst, especially over silica and alumina supports, is also reported to have a good stability against temperature changes (Ferreira-Aparicio et al., 2005). These results suggest that cobalt catalyst is a potential alternative among non-noble metal catalyst with a small amount of carbon deposition.

In terms of support, Ni and Co metals are usually supported on various oxide systems. Two kinds of oxides, reducible (CeO_2 , Nb_2O_5 , Ta_2O_5 and ZrO_2) and irreducible (Al_2O_3 , La_2O_3 , MgO and SiO_2) were used as supports (Wang and Ruckenstein, 2000). Among the irreducible metal oxides, Al_2O_3 , La_2O_3 and MgO provided stable catalytic activities during the period of study, and the activity increased in sequence. It was found that MgO and Al_2O_3 are the most promising supports; they provided a stable high activity with a CO yield of 83 to 85% and H_2 yield of 76 to 79% (Wang and Ruckenstein, 2000). In addition, studies using CaTiO_3 and BaTiO_3 perovskites containing a small amount of Ni in Ti sites as the precursor to obtain highly dispersed and stable nickel metal in situ, the results show high activity and resistant to coking (Hayakawa et al., 1999).

Table 2.2 shows the summary of previous research works related to the methane dry reforming and its significant results.

Table 2.2: Summary of previous research and its significant result

Catalyst	Significant results	Reference
Nickel catalysts supported on $\text{CaO} \cdot 2\text{Al}_2\text{O}_3$	- Nickel catalyst with different nickel loadings supported on nanocrystalline calcium aluminate employed in methane reforming, show high activity and stability due to presence of CaO in the support which declined coke deposition in catalysts.	(Ranjbar & Rezaei, 2012b)

	- 7% N loading show higher activity and lower coke formation.	
Co and Ni supported on CeO ₂ as selective bimetallic catalyst	- Bimetallic Co-Ni/CeO ₂ catalysts is more active, selective and thermally stable for the synthesis gas production due to intrinsic property of Co-Ni alloy.	(Luisetto et al., 2012)
Ni/perovskite catalysts prepared by solid phase crystallization method	- The catalysts, spc-Ni/MgTiO ₃ , spc-Ni/CaTiO ₃ , spc-Ni/Ca _{0.8} Sr _{0.2} TiO ₃ , spc-Ni/SrTiO ₃ , spc-Ni/Ca _{0.8} Ba _{0.2} were obtained in situ by the spc method.	(Hayakawa et al., 1999)
	- Ni/Ca _{0.8} Sr _{0.2} TiO ₃ and Ni/BaTiO ₃ catalysts showed high activity as well as high sustainability among the catalysts tested.	
Nickel catalyst supported on (Al ₂ O ₃ , CeO ₂ , La ₂ O ₃ , ZrO ₂)	- The catalyst supported on ZrO ₂ showed the highest stable activity. - The catalyst supported on CeO ₂ has a relatively good activity but showed sign of deactivation after certain reaction time.	(Barroso-Quiroga & Castro-Luna, 2010)
Strontium carbonate supported cobalt catalyst	- Co-SrCO ₃ showed high tolerance to oxidative atmosphere under 1MPa, 1023K.	(Omata et al., 2004)
Ni/BaTiO ₃ -Al ₂ O ₃	- Ni/BaTiO ₃ showed poor stability and severe coke formation. - Ni/BaTiO ₃ -Al ₂ O ₃ has a higher dispersion of nickel and Ni _{32.4%} /BaTiO ₃ -Al ₂ O ₃ exhibited a high catalytic activity and excellent stability for lower temperature in dry reforming.	(Li et al., 2012)
Y ₂ O ₃ -ZrO ₂ supported on nickel catalyst	- The formation of surface oxygen vacancies in Y ₂ O ₃ -ZrO ₂ system increase in the interaction between nickel species and the surface oxygen vacancies, thus improve the methane conversion.	(Bellido & Assaf, 2009)

	- The best performance achieved by 5Ni8YZ catalyst, with load of 8%mol Y ₂ O ₃ .	
Barium and lanthanum incorporation to supported Pt and Rh on α -Al ₂ O ₃	- La incorporation induces a rate enhancement in conversion of methane to synthesis gas	(Ghelamallah & Granger, 2012)
Nickel catalyst supported on nanocrystalline calcium aluminates with different CaO/Al ₂ O ₃ ratio	- Nanocrystalline calcium oxides with different CaO/Al ₂ O ₃ ratio are suitable as the support of catalysis in dry reforming process. - Calcium aluminate due to its relatively high basicity and small particle size show high activity and stability. - CaO in the catalyst can reduce the carbon formation during the reaction. - CH ₄ and CO ₂ conversion decreased with increasing CaO/Al ₂ O ₃ ratio, this may due to fact that higher ratio have lower surface area and thus lower nickel dispersion in catalysts.	(Ranjbar & Rezaei, 2012a)
CaO promoted Ni/ZrO ₂	- CaO-ZrO ₂ solid solution support suffers the influence of surface oxygen vacancies on their reduction behaviour. - The best performance achieved by 5Ni8CZ with CaO 8 mol% in support. - The addition of alkaline earth oxides, CaO to oxide supports for Ni catalysts improve reforming reactions by preventing carbon deposition on the active sites.	(Bellido et al., 2009)
Potassium promoted Ni/Al ₂ O ₃	- The addition of low amount of potassium (0.2%K ₂ O) increase catalytic activity (over 63% methane conversion) and low coke deposition (< 30mgC/g.cat)	(Juan-Juan et al., 2006)
Ni/La ₂ O ₃ /Al ₂ O ₃	- The species and amount deposited on the catalysts depended on size	(Xu et al., 2009)

	of Ni particles and texture of supporter.	
	- Metallic Ni particles <15nm can effectively suppress the formation of carbon filaments and thus decrease the amount of carbon deposition.	
Alumina supported on Pt, Ni and PtNi alloy	- The alloy formation is associated with higher activity and lower production of carbonaceous materials. - PtNi catalyst which is enriched at the surface by Pt has smaller metal crystal size than the onometallic Pt and Ni.	(García-Diéguez & Pieta, 2010)
La _{0.8} Sr _{0.2} Ni _{0.8} M _{0.2} O ₃ perovskite (M=Bi, Co, Cr, Cu, Fe)	- LNS (Cu) O perovskite possessed good performance in initial activity. - LNS (Fe)O showed high final activity and thermal stability with no carbon formation	(Sutthiumporn et al., 2012)
Ni/Al ₂ O ₃ and Ni/MgO-Al ₂ O ₃	- All the catalyst showed high activity towards dry reforming of methane. - The MgAl ₂ O ₄ spinel layer that formed over Ni/MgO-Al ₂ O ₃ can effectively suppress the phase transformation to form NiAl ₂ O ₄ spinel phases and can stabilize the Ni crystallite	(Guo et al., 2004)
Ni-Pd bimetallic catalyst on various support	- The catalytic activity decreases in the following ranking ZrO ₂ -La ₂ O ₃ . La ₂ O ₃ >ZrO ₂ >SiO ₂ >Al ₂ O ₃ >TiO ₂ - Bimetallic is more active than Ni and Pd alone. - A Ni to Pd ratio of 4 at metal loading of 7.5wt% showed the best result.	(Steinhauer et al., 2009)
NiMg/Al ₂ O ₃ nanocatalyst synthesized by reverse microemulsion method	- Proved to be a promising catalyst due to its high activity and stability. - Mg incorporation to Ni/Al ₂ O ₃ catalysts improves the Ni	(García-Diéguez et al., 2012)

	dispersion by the surface rearrangement and further reduces the carbon formation.	
SBA-15 supported nickel promoted by $\text{Ce}_{0.75}\text{Zr}_{0.25}\text{O}_2$	- The CZ addition enhances the Ni/SBA-15 catalytic behaviour toward methane conversion between 600°C and 630°C.	(Albarazi et al., 2013)
	- It enhances the catalysts stability	
$\text{NiCeO}_2\text{ZrO}_2\text{MgAl}_2\text{O}_4$ with various composition	- Best dry reforming performances were achieved with catalyst compositions having low Ni (2 wt %), ZrO_2 (<1 wt %) and high CeO_2 (>3 wt %) content.	(Corthals et al., 2011)
Ni-Ce supported on a modified mineral clay with Al and PVA (polyvinyl alcohol)	- The catalysts present high CO_2 and CH_4 conversions with high performances to H_2 and H_2/CO ratios between 0.6 and 1.2	(Daza et al., 2009)
$\text{Ni}_{0.1}\text{Mg}_{0.9}\text{O}$ nanocrystalline powder	- Highly stable activity for the reforming of methane with carbon dioxide.	(Zanganeh et al., 2013)
	- Surfactant addition has a significant effect on the textural properties of $\text{Ni}_{0.1}\text{Mg}_{0.9}\text{O}$ powders and led to obtain a powder with high surface area.	
Dealuminated FAU type Y and BEA zeolites supports on Ni and Pt (1 or 0.5 wt %)	- Dealumination by steaming of FAU type Y and BEA zeolites formed mesopores causing the metals to highly disperse during impregnation.	(Pinheiro et al., 2009)
	- The catalytic performance in the reforming showed that Ni-containing monometallic samples were inactive in the reaction due to the large amount of filamentous amorphous carbon deposited on these solids.	

2.6 Catalyst Preparation

Solid catalysts are highly sophisticated products derived from chemicals by means of several different procedures. The catalytic properties of heterogeneous catalysts are strongly affected by every step of the preparation together with the quality of the raw materials. The choice of a laboratory method for preparing a given catalyst depends on the physical and chemical characteristics desired in the final composition (Perego and Villa, 1997).

The criteria for a good catalyst depend on the activity, selectivity, thermal and mechanical properties, stability, morphology and cost (Rojas, 2013). The preparation of supported catalysts aims to attach the active phase onto the support. Impregnation, co-precipitation, homogeneous deposition, deposition of surfactant (organic agent) stabilized metal particles are some method in preparation of catalyst (Rojas, 2013). The general steps in preparation of catalysts start with mixing solution/solids, then equilibration or aging. After that solid liquid separation and drying. Calcination is carried out to decompose the metal precursor with formation of oxide and removal of gaseous products such as water and carbon dioxide (Perego and Villa, 1997). Finally, before the catalyst is ready to be used in any reaction, it must be activated.

Impregnation is the simplest method to prepare supported catalysts. Solution containing the metal precursor is contacted with porous support. For dry impregnation (pore volume impregnation), the exact amount of liquid to fill the pore volume of the support is used; as for wet impregnation, the amount of liquid depends on the solubility of the metal precursor. The electrostatic forces control the adsorption mechanism of the porous support (Rojas, 2013).

Previous studies show how calcium aluminate supported catalysts was prepared by using excess-solution impregnation method using prepared support and different concentrations of aqueous solutions of $\text{Ni}(\text{NO}_3)_2 \cdot 6\text{H}_2\text{O}$ to obtain 5, 7, 10 and 15 wt. % nickel content. After impregnation, the samples were dried at 80°C for 24 h and calcined at 600°C for 4 h (Ranjbar & Rezaei, 2012b).

Another study shows Ni-Ce catalysts supported on modified mineral clay were prepared by the incipient co-impregnating method using an exact quantity of $\text{Ni}(\text{NO}_3)_2 \cdot 6\text{H}_2\text{O}$ (10%